Earth's Future

RESEARCH ARTICLE
10.1029/2022EF002700

Special Section:
Advancing flood characterization, modeling, and communication

Spatiotemporal Characteristics of US Floods: Current Status and Forecast Under a Future Warmer Climate

Zhi Li[1], Shang Gao[1], Mengye Chen[1], Jonathan J. Gourley[2], and Yang Hong[1]

[1]School of Civil Engineering and Environmental Science, University of Oklahoma, Norman, OK, USA, [2]NOAA National Severe Storms Laboratory, Norman, OK, USA

Key Points:

- Overall increase in rainfall and flood occurrences and spatial scales over the continental US under a warmer climate
- There are weakening extreme rainfall and flood seasonality in the future
- Earlier and faster snowmelt exacerbates future floods in the West while drier antecedent soil moisture delays and offsets floods in the East

Supporting Information:

Supporting Information may be found in the online version of this article.

Correspondence to:

Y. Hong,
yanghong@ou.edu

Citation:

Li, Z., Gao, S., Chen, M., Gourley, J. J., & Hong, Y. (2022). Spatiotemporal characteristics of US floods: Current status and forecast under a future warmer climate. *Earth's Future*, *10*, e2022EF002700. https://doi.org/10.1029/2022EF002700

Received 3 FEB 2022
Accepted 7 JUN 2022

Author Contributions:

Conceptualization: Shang Gao, Yang Hong
Data curation: Zhi Li
Formal analysis: Zhi Li
Funding acquisition: Yang Hong
Investigation: Zhi Li
Methodology: Zhi Li, Shang Gao, Mengye Chen, Jonathan J. Gourley
Project Administration: Yang Hong
Software: Zhi Li

Abstract Floods in the US exhibit strong spatiotemporal variability, mainly controlled by precipitation types and catchment attributes. In a future warmer climate, it remains largely unclear how such features change, relative to the current climate. Global Climate Models at coarse resolution cannot resolve convective-scale storms which is one of the major weather systems causing devastating floods in the US. Alternatively, coupled, high-resolution and continental-scale climate and flood simulations can advance our understanding. In this study, we couple a 4-km convection-permitting climate simulation model with a 1-km hydrologic model to simulate the spatiotemporal variability of rainfall and flooding over the contiguous US. In particular, changes in rainfall and flood frequency, spatial scale, and seasonality are explored in major climate divisions. We found: (a) an overall increase in flood frequency (+101.7%) and spatial extent (+44.9%), mainly attributed to more extreme rainfall and variability in the future; (b) weakening rainfall and flood seasonality, resulting in more random and unpredictable events throughout the year; (c) earlier flooding season onsets in the West and snow-dominated regions while delayed onsets in the East driven by drier antecedent soil moisture; (d) correlation between extreme rainfall and flood onsets is becoming stronger in the West yet weaker in the East in the future. Findings in this study can potentially serve as a basis for future flood exposure and risk assessments, as well as more scientific understanding of changing flood-generating mechanisms across the CONUS.

Plain Language Summary Floods are one of the most devastating water-related natural hazards in the world. With more frequent and severe extreme events in the future, accompanied by a growing population settled in the floodplains and aging infrastructures, flood risks are becoming much higher than the current situation. In this study, we attempt to characterize the spatiotemporal impact of future floods over the continental United States. In particular, we focus on the thermodynamic impacts of future storms fueled by higher temperature and atmospheric moisture. The projected changes can not only help assess flood risks and exposures in the future but also advance our understanding of changing flood-generating mechanisms across the US.

1. Introduction

Population and assets exposed to floods have been ever-increasing over the globe (Hirabayashi et al., 2013; Jongman et al., 2012; Tellman et al., 2021). Changes in land use have shifted so the United States is the leading country with the highest exposed asset values (Jongman et al., 2012; Rajib et al., 2021). Continuing urbanization, aging infrastructures, and intensified storms can exacerbate the current situation.

Future flood changes are often quantified by frequency (Hirabayashi et al., 2013; Li et al., 2022; Swain et al., 2020), magnitude (Bates et al., 2020; Brunner et al., 2021), and spatiotemporal characteristics (Alfieri et al., 2020; Tellman et al., 2021) with greater attention on the former two. Flood spatiotemporal features, spatial scale and seasonality in particular, are especially central to anticipating flood exposure and risk management (Blöschl et al., 2017; Jongman et al., 2012; Tellman et al., 2021). Moreover, they are recognized as attributes to generalize flood-generating mechanisms (Brunner et al., 2020; Li, Chen, Gao, Gourley, et al., 2021; Merz et al., 2021; Smith et al., 2011; Stein et al., 2021; Villarini, 2016). A body of studies has successfully described US flood spatial dependence and seasonality based on historical observations (Brunner et al., 2020; Li, Chen, Gao, Gourley, et al., 2021; Stein et al., 2021; Villarini, 2016). Villarini (2016) completed a comprehensive study on US streamflow seasonality, in which he did not observe strong temporal shifts in flood seasonality, but seasonality strength is weakening due to human interference. Berghuijs et al. (2019) proposed the term "flood synchrony scale" to characterize the flood extent of which at least half of the river gauges co-experience floods. Brunner

Supervision: Jonathan J. Gourley, Yang Hong
Validation: Zhi Li
Visualization: Zhi Li, Mengye Chen
Writing – original draft: Zhi Li
Writing – review & editing: Zhi Li, Shang Gao, Mengye Chen, Jonathan J. Gourley, Yang Hong

et al. (2020) applied this concept in US river gauges and identified 15 regions with similar flood behaviors. Nonetheless, the aforementioned studies have provided little understanding outside gauge locations that are sparsely sampled over the US To fill the gap, continental-scale hydrologic simulations at each river reach are essential. Moreover, continuous simulation in lieu of event-based simulation is critical as the antecedent catchment condition can thus be well represented (Wasko et al., 2019).

However, changes in future spatiotemporal flood characteristics are more equivocal, although some generic features such as earlier snowmelt season are generally expected. Primary challenges hindering additional insights are: (a) the lack of high-resolution climate simulations underpinning fine-scale flood simulations, especially for flood extent, (b) uncertain climate simulations that often require large ensemble predictions to replace the traditional one-model-one-vote approach (Clark et al., 2016; Giuntoli et al., 2021), and (c) complex flood-generating mechanisms (Wasko et al., 2019). For (a) and (b), these challenges persist to date, but workarounds have been proposed. For instance, downscaling Global Climate Models (GCM) has been explored over the last two decades to enable regional climate projections. Generally, two downscaling approaches have become mainstream: statistical downscaling and dynamic downscaling (the predictor-predict approach). Non-stationarity in atmospheric components has been the obstacle for statistical downscaling and is yet to be resolved by the community. Likewise, future flood characteristics are unlikely to remain stationary since the atmosphere is the main driver for floods. In contrast, dynamic downscaling uses the outputs from the GCMs and then drives a regional climate model, yielding more realistic simulations. Lately, dynamic downscaling has been prevailing and holding great promise owing to the increased computational power and physics parameterizations (Clark et al., 2016; Liu et al., 2017; Prein et al., 2017). The recent CONUS-1 data set (Liu et al., 2017), produced at hourly and 4-km resolution, has become one of the highest resolution continental climate simulations, which has empowered a wide range of regional climate studies, including extreme precipitation (Prein et al., 2017), snowmelt (Musselman et al., 2018), flash flood-producing storms (Dougherty & Rasmussen, 2020), flood frequency analysis (Yu et al., 2020), etc. By applying the Pseudo Global Warming (PGW) approach (Schär et al., 1996), this data set circumvents the more uncertain dynamic changes yet focuses on more deterministic thermodynamic changes. As such, it is suited for continental flood simulations requiring high resolution and broad spatial coverage.

The focus on underlying physical processes recognizes that floods are not only dependent on extreme rainfall, for which there is high confidence in increases over North America in the future (Douville et al., 2021), but with modulations by the land surface processes (Merz et al., 2021). Undoubtedly, increasing rainfall extremes will directly amplify flood magnitude in a controlled environment (meaning other variables remain unchanged). However, there is widespread evidence that antecedent catchment conditions (soil moisture and groundwater level) are becoming drier as temperature rises in conjunction with more partitioning of snowfall to rain and earlier snowmelt (Ivancic & Shaw, 2015; Sharma et al., 2018; Wasko et al., 2021). These conditions counteract increases in extreme rainfall magnitudes to modulate the flood-generating process. While there are so many conceptual discussions in the literature, there are still ongoing works perceiving extreme precipitation as a proxy for high streamflow (Ivancic & Shaw, 2015). Moreover, many details are lacking about which processes dominate and for which times of the year and climate divisions.

Motivated by the lack of continental-scale studies of reach-level flood characteristics beyond gauge locations and elusive future changes of such, in this study we seek to address the following objectives: (a) assess the relative influences of atmospheric and land surface drivers to flood spatiotemporal characteristics by comparing present-day conditions to future ones, (b) quantify the spatial changes in rainfall and flood extents, and (c) estimate temporal shifts and changes of the seasonality of rainfall and flooding in the CONUS. We achieve these goals via simulating US reach-level streamflow using forcing data from the outputs of a continental convection-permitting climate model. Methodologies are then developed to quantify rainfall/flood spatial scales after spatiotemporal clustering. To our best knowledge, we, for the first time, analyze the spatiotemporal changes in continental convective-scale rainfall and kilometer-scale floods based on a proposed framework that works for distributed models. It is anticipated that this study provides a practical assessment of US extreme flood characteristics, and more importantly, on their future changes so that local communities can be well prepared to mitigate their impacts.

2. Data and Methods

2.1. US Climate Divisions

Statistical results throughout this study are aggregated to US climate regions to provide a more holistic view. The popular Koppen-Geiger climate classification, used widely in climatological studies, however bears inhomogeneous divisions in the US For instance, the Southwest, representing an arid climate, is divided into four sub-classes, while the vast southeastern US is represented by a single class, as shown in Figure S1a in Supporting Information S1. In contrast, the Bukovsky climate division in Figure S1b in Supporting Information S1 equally divides the US into 17 classes based on temperature and precipitation (Bukovsky, 2011). This climate regionalization yields subdivisions with similar areas and is thus preferred in this study as well as in other climate studies (Prein et al., 2017). A list of data used in this study can be found in Table 1 in Supporting Information S1.

2.2. Convective-Permitting Climate Simulation

In this study, we use the outputs from a 13-year CONUS climate simulation at hourly time step and 4-km grid spacing to force a continuous hydrologic simulation. The retrospective simulation control run (CTL) from 2000 to 2013 downscales ERA-Interim reanalysis data, with spectral nudging applied (Liu et al., 2017). In parallel, a future climate counterpart is simulated by applying the Pseudo Global Warming approach (PGW) which perturbs climatic boundary conditions (e.g., wind, temperature, humidity, and sea surface temperature) from an ensemble mean of 19 CMIP5 models under the Representative Concentration Pathway (RCP) 8.5. Climatic changes are evaluated by subtracting each variable in the simulation period 2071–2100 from the reference period 1976–2005. This approach highlights relative changes and minimizes the absolute uncertainties. The essence of the PGW run is to assess more deterministic thermodynamic climate change impacts while not allowing the impacts of more uncertain dynamic changes. Because of spectral nudging, we can then conduct event-to-event analysis of rainfall and floods based on the current and future climate.

2.3. Hydrologic Simulation

The Coupled Routing Excess STorage (CREST) V2.1 is used in this study to simulate hydrologic responses to climate change. The CREST model is a distributed hydrologic model that couples Snow-17 for snowmelt, Variable Infiltration Curve (VIC) for soil infiltration, and kinematic wave solution for overland and channel routing. A conceptual linear reservoir routing is used for subsurface flows. Prior studies have successfully applied the CREST model for operational flash flood forecasts in the US (Gourley et al., 2017), detecting global floods and landslides (Wu et al., 2012; Zhang et al., 2016), mapping flood inundation extents and depths (Chen et al., 2021; Li, Chen, Gao, Luo, et al., 2021), and simulating the water cycle (Li et al., 2018). Building upon a previous legacy that operates the CREST model for real-time flash flood forecasting (Flamig et al., 2020; Gourley et al., 2017; Vergara et al., 2016), we use the a-priori distributed parameters over the CONUS. Since potential evapotranspiration (PET) in the future will increase given global warming, we calculated future daily PET based on the Thornthwaite equation that depends only on daily temperature from climate simulations (Thornthwaite, 1948). Other variables such as hourly precipitation and temperature are direct inputs to the CREST model. We simulated hourly streamflow at 1-km grid spacing from 2001 to 2013, with the first year used to warm up the model states.

2.4. Rainfall/Flood Spatial Scale

Rainfall spatial scale is measured in this study by first considering the contour lines of daily rainfall enclosed by a certain extreme threshold, referred to as the areal extent (Figure 1). In practice, we plot contour lines for daily rainfall greater than 2-year average recurrence interval thresholds for the retrospective simulation. The use of 2-year rainfall as thresholds can be found in the literature such as Lamjiri et al. (2017). A gamma distribution is fitted to the annual maximum rainfall values, and a certain value exceeding the 2-year return interval is determined from the distribution. The goodness-of-fit test (Anderson-Darling test) regarding extreme value distribution is shown in Figure S2 in Supporting Information S1, where 92% of the samples pass the significance

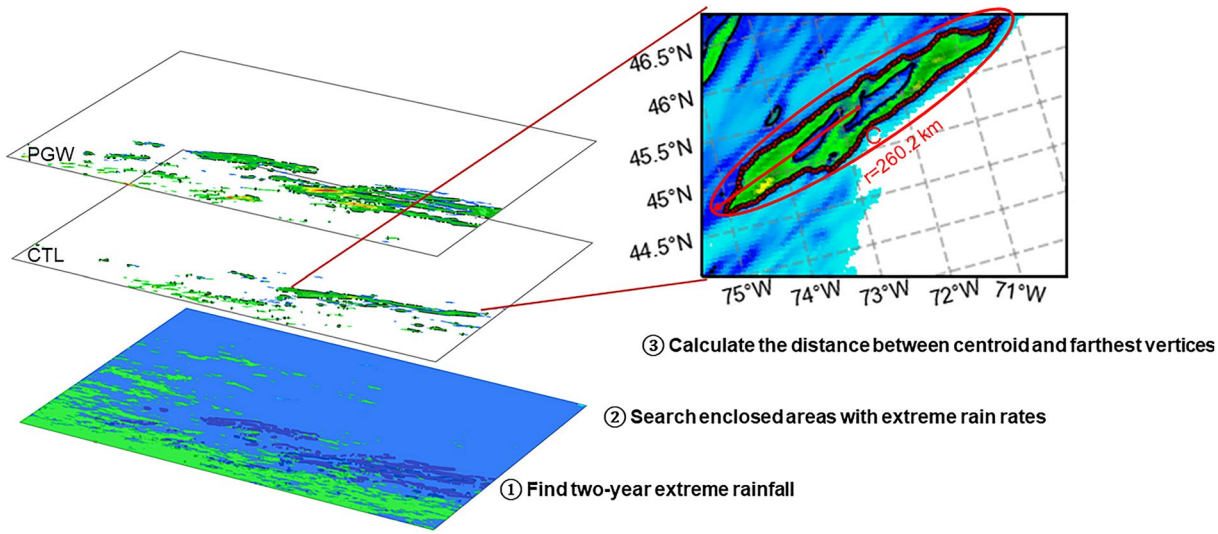

Figure 1. An illustration of rainfall spatial scale calculation, where symbol *C* represents the enclosed curve. CTL: historical simulation; Pseudo Global Warming: future simulation.

test at a significant level of 0.01. Then, we sample vertices along the contour line. The area can be approximated numerically using Green's theorem shown in Equation 1:

$$A = \iint \mathrm{d}A = \frac{1}{2}\oint_C x\mathrm{d}y - y\mathrm{d}x, \tag{1}$$

where C is a closed curve that bounds regions with extreme rainfall, and x, y refer to the coordinate of the vertices sampled along the contour line. Lastly, the rainfall spatial scale is computed by measuring the distance between the centroid of the enclosed area and the farthest point on curve C. For the example given in Figure 1, the 2-year rainfall threshold in such a region is 28.6 mm/day, and the area of an enclosed curve is calculated as 3,211 km^2 using Equation 1. The spatial scale of this event is 260.2 km.

River flooding in nature, unlike continuous rainfall fields, occurs along elevation-dependent river networks. Therefore, a different strategy needs to be developed to account for river network topology. Flood spatial scale, by definition, is the maximum spatial extent in which multiple gauges or reaches co-experience flooding synchronously. Berghuijs et al. (2019) proposed the measure of flood synchrony scale by computing the maximum radius of gauges within which at least 50% of them are flooded. Similar approaches have been adopted in the literature (Brunner et al., 2020; Kemter et al., 2020). However, their works are limited to gauge sites that are sparsely distributed, and there lacks a detailed representation of river topology. As a consequence, the flood synchrony scale may be overestimated by disconnected river networks. In contrast, distributed hydrologic simulations can overcome this limitation by incorporating pixel-wise sampling with a river network embedded in the model setting. A challenge notwithstanding for distributed models in flood synchrony studies is that there is no prior standard to calculate flood spatial scale.

In this study, we propose a method that fills this gap and can be applied in any distributed streamflow simulation. First, the flood threshold is computed based on an N-year event. Here "N" can be replaced with any number by considering the length of data and application. In this study, given the total 10-year simulation, we select a 2-year streamflow value as the threshold, which is approximated as a bankful condition for river channels (He & Wilkerson, 2011). Similar to 2-year rainfall, a log-Pearson type III distribution is fitted to the annual maxima streamflow values, which is a conventional way to calculate return intervals by the US Geological Survey (Veilleux et al., 2014). The goodness-of-fit test (Anderson-Darling test) of the distribution is shown in Figure S3 in Supporting Information S1, where 91.6% of the samples pass the significance test at a significant level of 0.01. With the flood thresholds available at all grid cells, flood occurrences at each pixel can be estimated by simply counting the events that exceed this threshold. Second, the flood occurrences can be rearranged in a matrix form ($m \times n$) with binary values, termed the

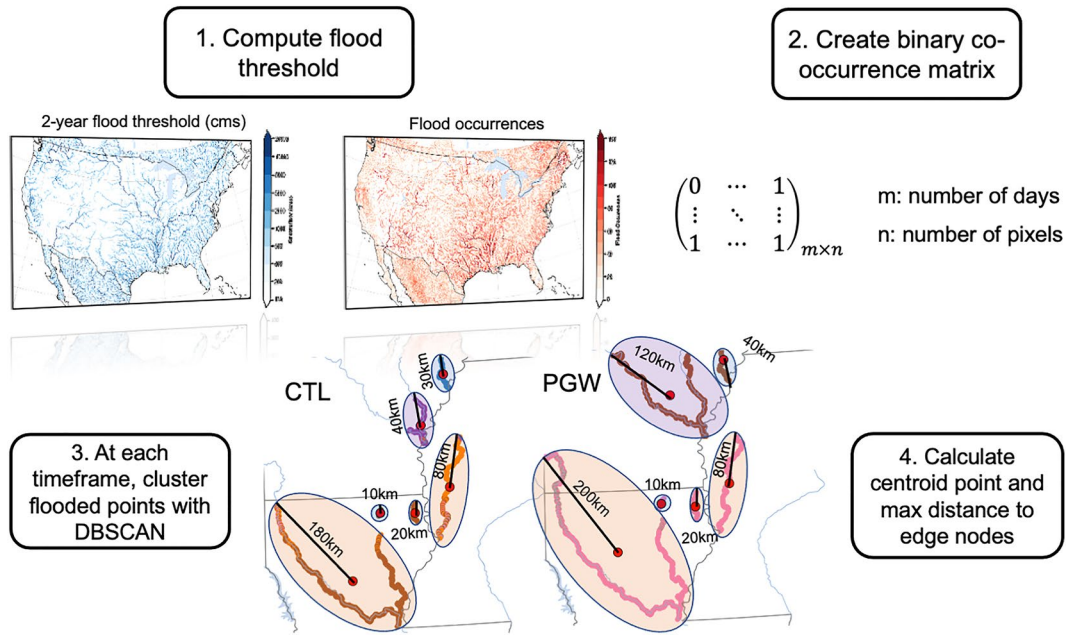

Figure 2. Schematic view of calculating flood spatial scale.

co-occurrence matrix. Here "*m*" represents the number of days or hours, depending on the data frequency, and "*n*" represents the number of pixels in output streamflow simulation. The co-occurrence matrix is used to select synchronous flood events and cluster pixels in proximity. Third, at each timestamp, we cluster flooded pixels with an unsupervised machine learning algorithm, Density-Based Spatial Clustering of Applications with Noise (DBSCAN) (Ester et al., 1996). The DBSCAN is a density-based clustering non-parametric algorithm that groups high-density points in space and marks isolated points as outliers. In doing so, we can remove isolated flood pixels while focusing on densely flooded regions. Lastly, we find the centroid geophysical location within each cluster and compute the maximum distance to enclosed edge nodes. A schematic flowchart of these processing steps is shown in Figure 2. Similar approach can be found in Brunner et al. (2020).

2.5. Flood Seasonality Measures

We aggregate the hourly streamflow data to daily to investigate flood seasonality over the CONUS. The circular statistics (i.e., circular mean, circular variance) are used for data such as flood calendar days on a polar coordinate system (Burn, 1997; Villarini, 2016). Circular mean and resultant length are the two primary measures to determine the average rainfall/flood days in Days of the Year (DOY) and strength of the seasonality, respectively. The strength of seasonality reflects how strong the seasonality is, with one indicating a strong seasonal cycle and 0 indicating no seasonal cycle. For brevity, we term the strength of seasonality as the seasonality index (SI) hereafter. Equations 2 and 3 express the calculation of circular mean and SI in a complex domain.

$$\text{Mean} = A\left(\sum_{j=1}^{n} \exp\left(i \cdot \alpha_j\right)\right) \tag{2}$$

$$\text{SI} = \frac{1}{N} \left\| \sum_{j=1}^{n} \exp\left(i \cdot \alpha_j\right) \right\| \tag{3}$$

where function A returns the angle of the complex; i is the imaginary unit; α_j is the jth day of the year with a range of (0.365). The $\| \cdot \|$ denotes the absolute value.

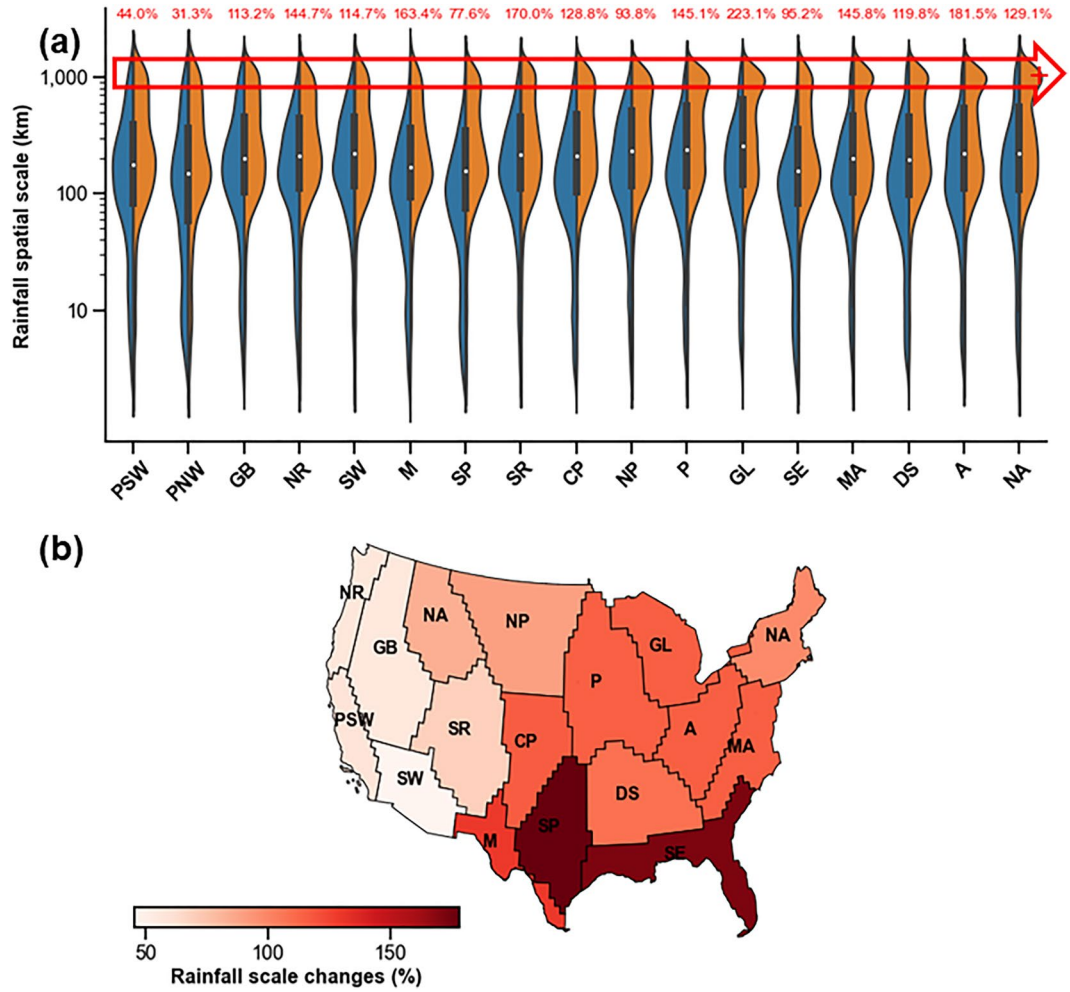

Figure 3. (a) Violin plot of current and future rainfall spatial scales grouped by the Bukovsky regions. Numbers in red text indicate relative changes (%) in extreme rainfall occurrences; (b) Map of rainfall spatial scale changes, averaged over the Bukovsky regions.

3. Results

3.1. Frequency and Spatial Changes

3.1.1. Extreme Rainfall

Extreme rainfall appears to increase both in occurrences (+118.0%) and spatial scales (101.7%) across all US climate regions under future climate simulation (Figure 3). Driven by different weather patterns, such changes vary by region. In the Pacific West Coast, the increases in both extreme rainfall occurrences and spatial scales are the least (+37.7%/58.4% for the change of occurrences/scale) among US climate zones. The main forcing agent there for extreme rainfall is atmospheric rivers (ARs) which are narrow and long plumes that originated from the tropics to replenish water resources and cause flooding along the West Coast. It is found that 78%–100% of the storms in the Pacific Northwest (PNW) are associated with ARs, although such fraction reduces to 60% in the Pacific Southwest (PSW) (Lamjiri et al., 2017). In a warmer climate, the dominant thermodynamic change leads to a 35% increase in AR frequency (Hagos et al., 2016), which is comparable to our results. The Southwest, influenced by the North American Monsoon (NAM), is projected to experience 114.7% more events and 45.6% greater scales. The Great Plains have been mainly impacted by mesoscale convective systems (MCSs) and tropical cyclones, which are expected to increase precipitation extremes owing to strengthened convective updrafts and intensified cyclone circulation in a warmer climate (Nie et al., 2018; Prein et al., 2017). We see on average a 99.9% and 128.1% increase in frequency and spatial scale, indicating that the increase in spatial scale outpaces

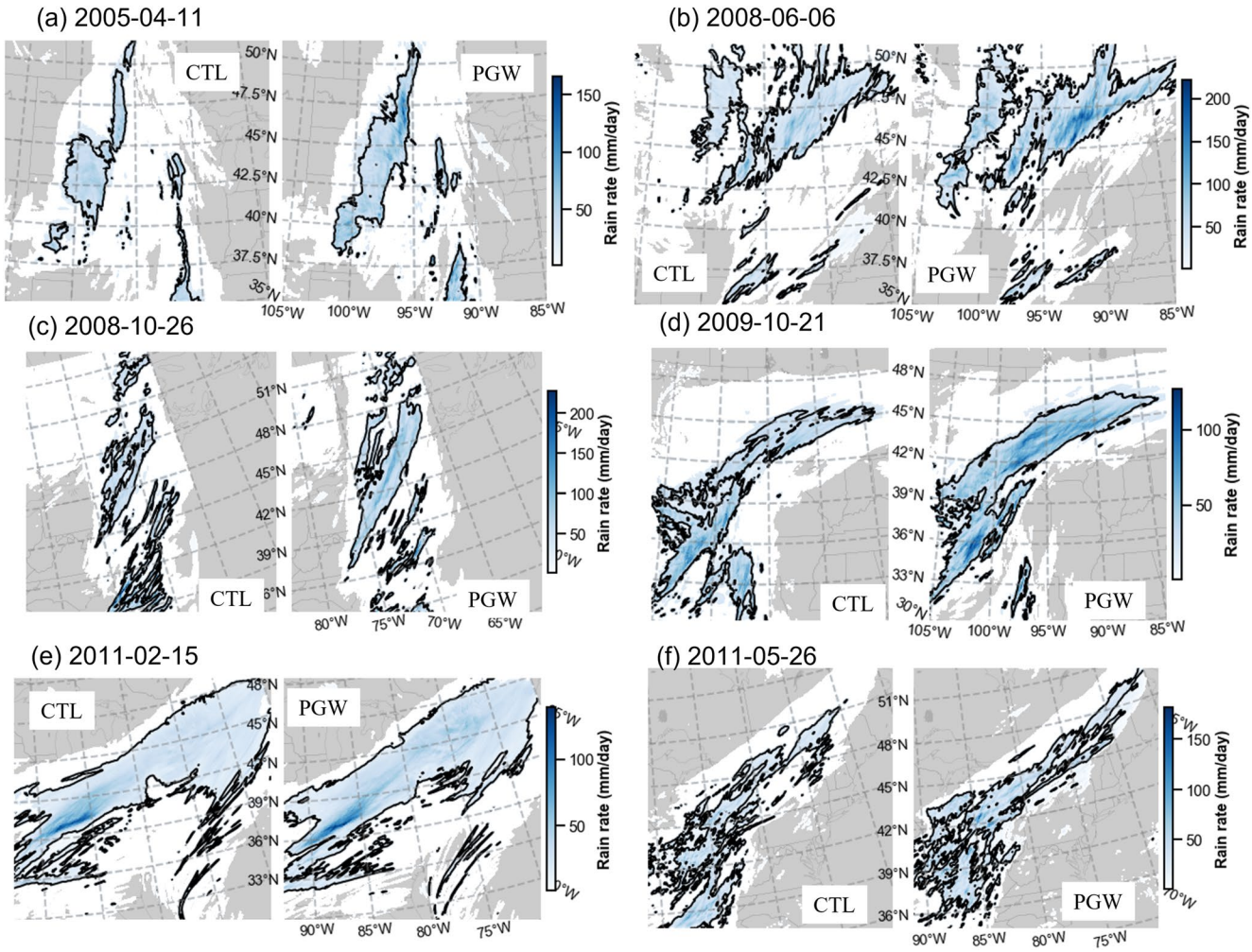

Figure 4. Maps of six storm events show the spatial scale difference between CTL and Pseudo Global Warming. The black contour line encloses the area whose rainfall rates exceed the 2-year rainfall threshold.

that in frequency. In the central US, where the MCSs contribute 30%–70% of the total warm-season precipitation (Feng et al., 2016; Fritsch et al., 1986), extreme rainfall occurrences (167.4%) are the mostly increased among climate divisions. The East Coast, influenced by tropical and extratropical cyclones, has a 123.3% and 128.9% increase in frequency and spatial scale. The East Coast has the largest change in rainfall spatial scale, partly attributed to increased storm motion (Prein et al., 2017). In general, we observe an increasing rainfall spatial scale from the West Coast to the East Coast (Figure 3b), implying a transition from convective-scale to synoptic-scale storms in the future. Six individual storms in Figure 4 visually manifest the increase in rainfall spatial scale in PGW. Two factors result in the increase in spatial scale: (a) single storm grows in length in PGW run (Figures 4b and 4e); (b) individual storms in CTL are connected to become large storms in PGW (Figures 4a–4d, and 4f).

3.1.2. Floods

Roughly one-third of the extreme rains in the US translates to floods by comparing their occurrences in Figures 3 and 5, which is close to the ratio of 36% estimated by Ivancic and Shaw (2015) and Sharma et al. (2018). The increase in extreme rainfall and snowmelt overcome the drier catchment states under anthropogenic warming, resulting in an increase in flood frequency and spatial scales across the US climate zones in Figure 5.

Similar to the frequency changes of extreme rainfall, flood frequencies (scales) in Figure 5 are increased by 55.2% (45.9%) in the Great Plains. However, the central US is likely to experience 74.2% more frequent floods and 33.6% greater flood extent, much less than the changes in the western US The East Coast also sees a reduced

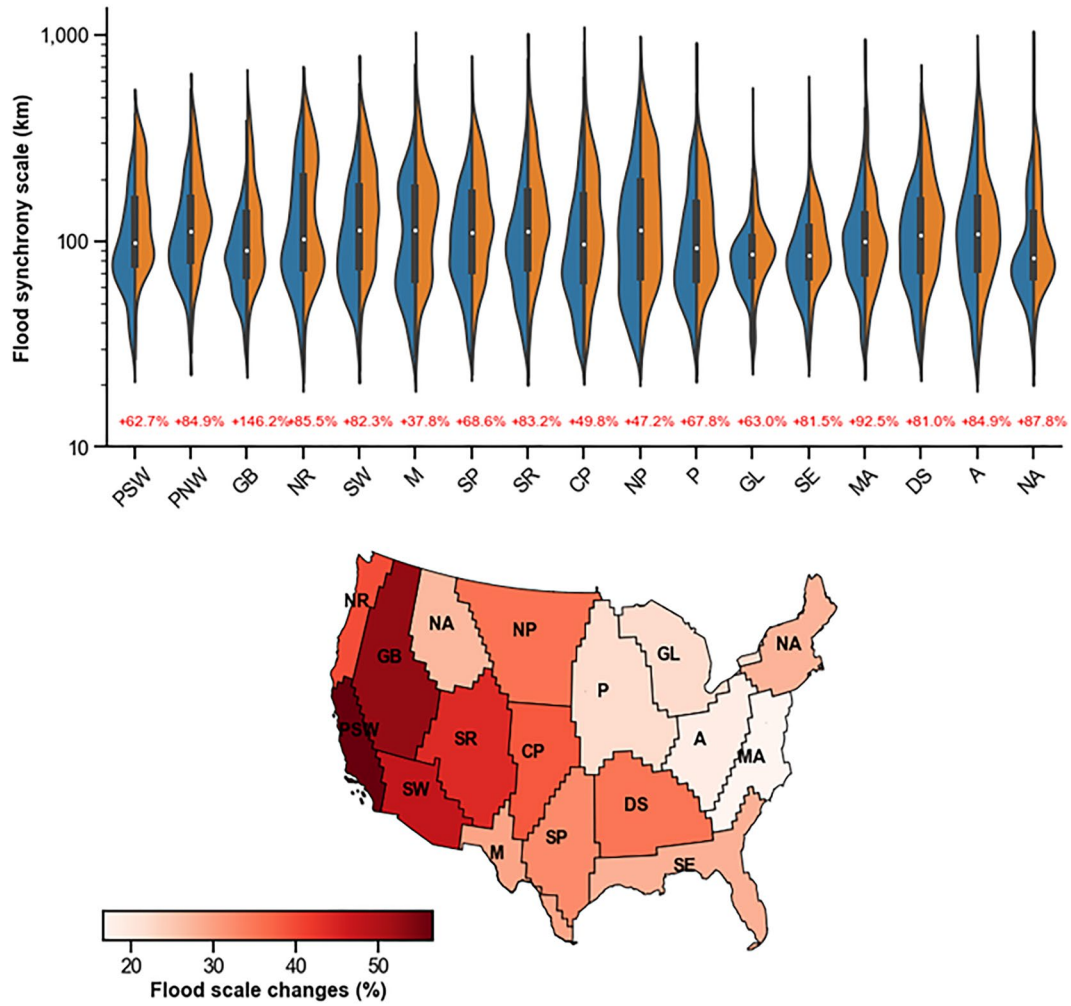

Figure 5. Similar to Figure 3, but for floods.

increase in flood spatial scale (35.8%) compared to the West Coast (70.6%). Relatively speaking, floods in the western US are becoming more severe in the future than those in the central and eastern US, opposite to rainfall changes. Such a pattern corroborates the multidisciplinary nature of flooding rather than being a pure atmospheric process. From the perspective of flood-generating mechanisms, the western US features steeper terrain and shallower soil profiles that more typically yield surface runoff by the infiltration excess process (i.e., rainfall rates exceed maximum soil infiltration capacity) and snowmelt (Brunner et al., 2020; Stein et al., 2021). The infiltration excess process is less dependent on catchment wetness (antecedent soil moisture or groundwater level) but rather on rainfall intensity. Increased surface water availability from snowmelt and rain on snow in a warmer climate apparently increase flood risk in the western US (Musselman et al., 2018). On the contrary, the relatively flatter terrain and deeper soil profiles in the central and eastern US yield runoff generation by the saturation excess process (i.e., surface runoff is produced after the soil saturates from the bottom up), thereby leaving floods sensitive to antecedent soil moisture and groundwater levels. These two hydrological states, however, are more likely to decrease in a warmer climate because of increased atmospheric temperature and PET (Sharma et al., 2018; Wasko & Sharma, 2017).

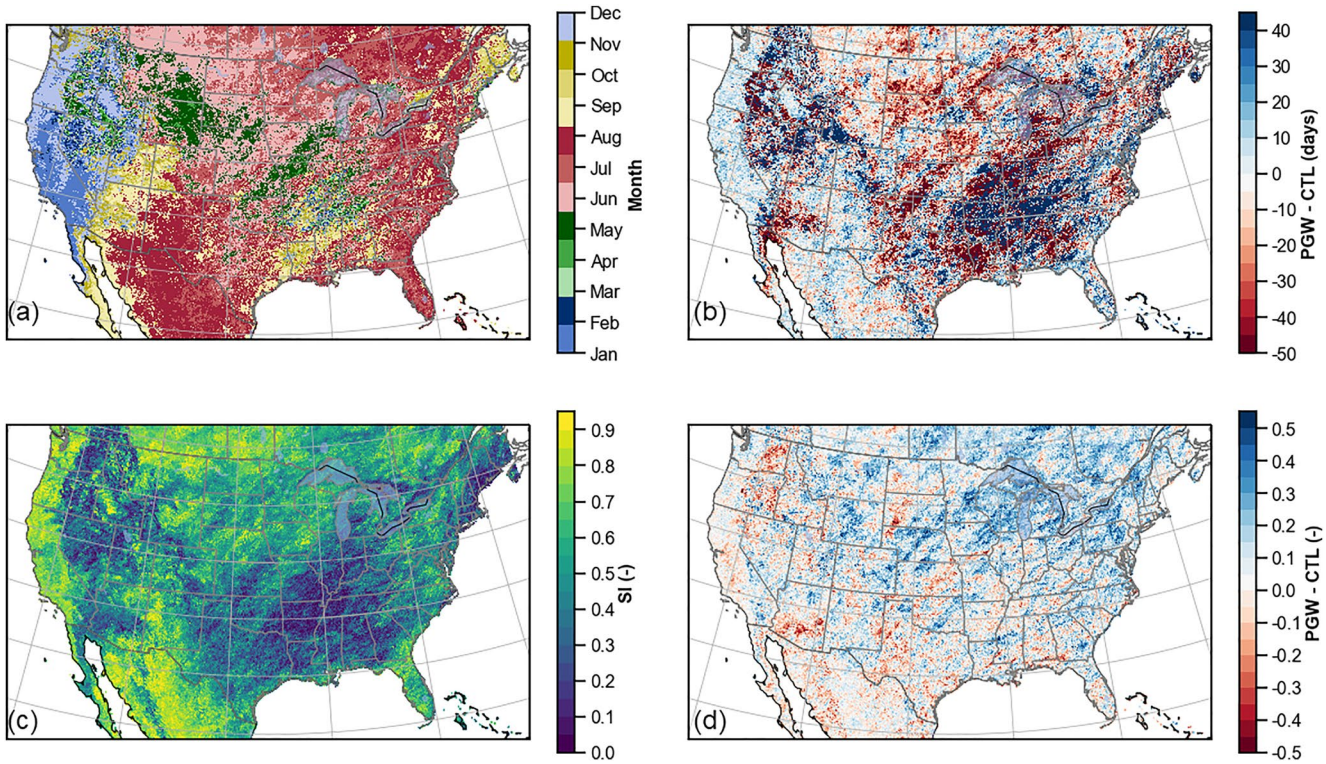

Figure 6. Maps of temporal changes of extreme rainfall: (a) retrospective rainfall seasonality (month); (b) difference of peak day between Pseudo Global Warming (PGW) and CTL; (c) rainfall seasonality index; (d) differences of seasonality index between PGW and CTL.

3.2. Seasonal Changes

3.2.1. Western United States

Figures 8 and 9 depict the seasonality of extreme rainfall simulated by CTL and its changes by taking the *DOY* difference (PGW minus CTL). Figures 6a and 7a, showing the spatial distribution of the months at which extreme rainfall occurs, are on par with US extreme rainfall climatology. The Pacific West Coast, as discussed in Section 3.1, is dominantly influenced by ARs that occur in winter (mostly in January). Therefore, the flood season in such a region, as shown in Figures 8a and 9a, follows closely with the extreme rainfall season. In fact, it is also the place that has the strongest rainfall/flood seasonality, with the SI of both rainfall and floods above 0.8. Future changes of peak days and seasonality index are marginal for both rainfall (Figures 7b and 7d) and floods (Figures 9b and 9d), with a small Inter-Quartile Range (IQR). Moving toward the East, SI values for both rainfall (Figure 7c) and floods (Figure 9c) tend to decrease with increasing IQR, pointing to more complex inland weather systems. Future SI values in the east of the Pacific Coast indicate negative changes in the future, manifesting weakening seasonal cycles of rainfall (Figure 7d) and flooding (Figure 9d). The Great Basin is jointly impacted by ARs, troughs, and cutoff lows (Prein & Mearns, 2021), leading to a more diverse seasonality of extreme rainfall (Figure 7a) and flooding (Figure 9a), yet centered in wintertime. Over the Northern Rockies, extreme rainfall or snowfall spans the winter-spring-summer season. Due to the large fraction of snowmelt, flood seasons are centered in late spring and early summer. Future floods are becoming, on average, 22 days earlier because of earlier snowmelt caused by increasing temperatures, comparable to the 3–5 weeks results by Xu et al. (2021). The Southern Rockies are featured by spring-summer-fall extreme rainfall and floods occurring during the warm season from spring through fall. Notably, flood seasonality (0.77) over the Rockies is much stronger than rainfall seasonality (0.53), which is attributed to the contribution of snowmelt that typically occurs in late spring and early summer. However, flood seasonality in such a region in the future will decrease by 0.23, a result of less snowmelt contributing to flooding generation from a decreasing snowpack. As a consequence, one can infer that the reduced flood seasonality complicates predictability in downstream snow-fed streams. The Southwest region

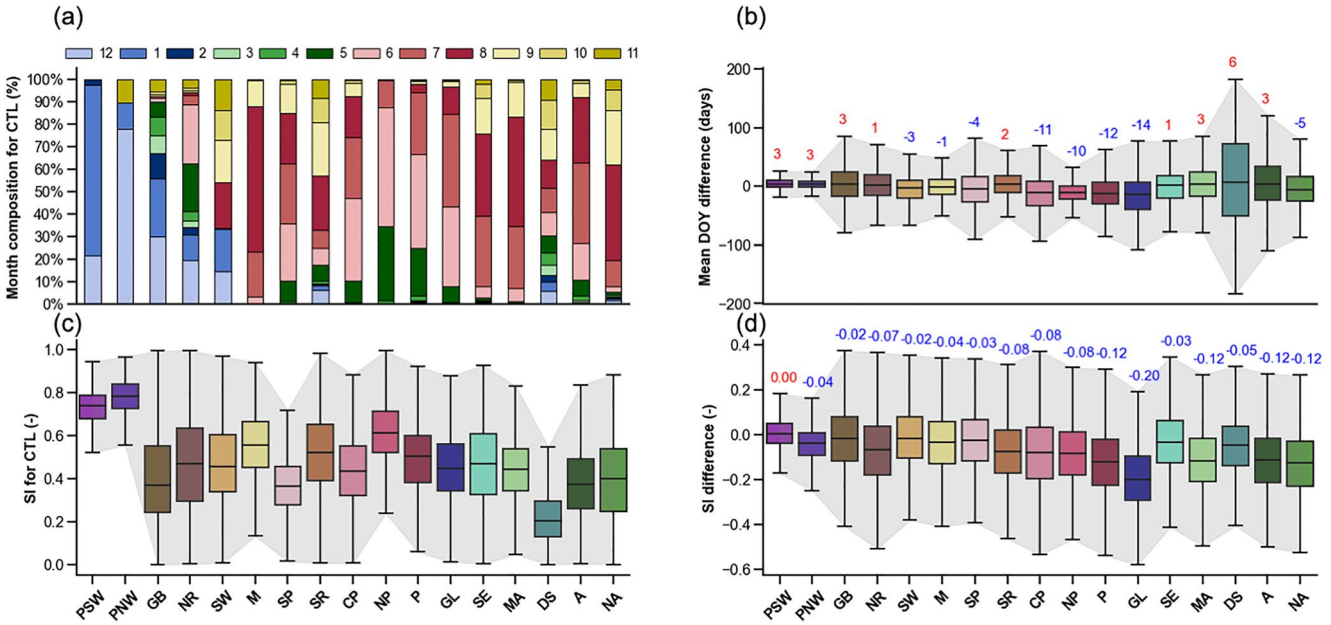

Figure 7. Retrospective rainfall seasonality and changes grouped by the Bukovsky regions. (a) month compositions in retrospective setting; (b) differences in Date Of Year between Pseudo Global Warming (PGW) and CTL; (c) seasonality index (SI); (d) differences of SI between PGW and CTL. The Inter-Quartile Range (defined as the upper and lower bound of the boxplot) is the shaded gray color. The numbers above the boxplot are the median values, which indicate increase (red) or decrease (blue) in seasonality.

is equally influenced by summer-fall NAM and winter inland-penetrating Pacific storms, while over half of the flood events occur in fall. However, no significant temporal shifts are observed in the future simulation.

3.2.2. Central United States

Weather types in the central US are composed of spring-summer MCSs (Ashley et al., 2003; Prein et al., 2017), summer-fall tropical cyclones (Chalise et al., 2021; Li, Chen, Gao, Gourley, et al., 2021), and spring extratropical cyclones (Barbero et al., 2019), among which extreme rainfall events in summer are the most prevalent (Figure 7a). Flood events in late spring are common in the northern plains (Figure 9a), mainly caused by the contribution from snowmelt and rain-on-snow events (Brunner et al., 2020; Villarini, 2016). Owing to earlier onsets of seasonal snowmelt (Figure 7b; Li, Chen, Gao, Gourley, et al., 2021), flood events in the Northern Plains, Great Lakes, and Prairie will become, on average, approximately 1 week earlier in the future (Figure 9b). Similar to the Rockies, the seasonality of extreme rainfall and flood in the central US is weakening in the future (Figures 7 and 9d), which makes flood prediction more challenging (Ledingham et al., 2019).

3.2.3. Eastern United States

Extreme rainfall in the eastern US is associated with cool-season extratropical cyclones and warm-season convective rainfall. The seasonality of rainfall on the East Coast reaches 0.6. Flood events, caused by convective rainfall and exacerbated by snowmelt in the Appalachians and New England, tend to span across seasons (Figure 7a). Flood seasonality in the eastern US is 0.3 (Figure 9b). As discussed in Section 3.1.2, flood generation is tied to catchment states in these regions, meaning rainfall exerts a less important role than that in the western US. Due to drier antecedent states (e.g., soil moisture and groundwater level), flood events will be delayed for tens of days in a warmer climate (Figure 9b), especially for the Mid-Atlantic (14 days) and Deep South (10 days).

3.3. Temporal Correlation Between Rainfall and Floods

Despite decreasing rainfall and flood seasonality in the future, the circular correlation of event date between extreme rainfall and floods increases (Figure 10). This can be explained by less accumulating snowpack in the US which delays rainfall-runoff transformation. Similarly, the correlation of seasonality between rainfall and floods increases from 0.63 (CTL) to 0.77 (PGW). The seasonal cycle of rainfall and flooding diminishes in the future,

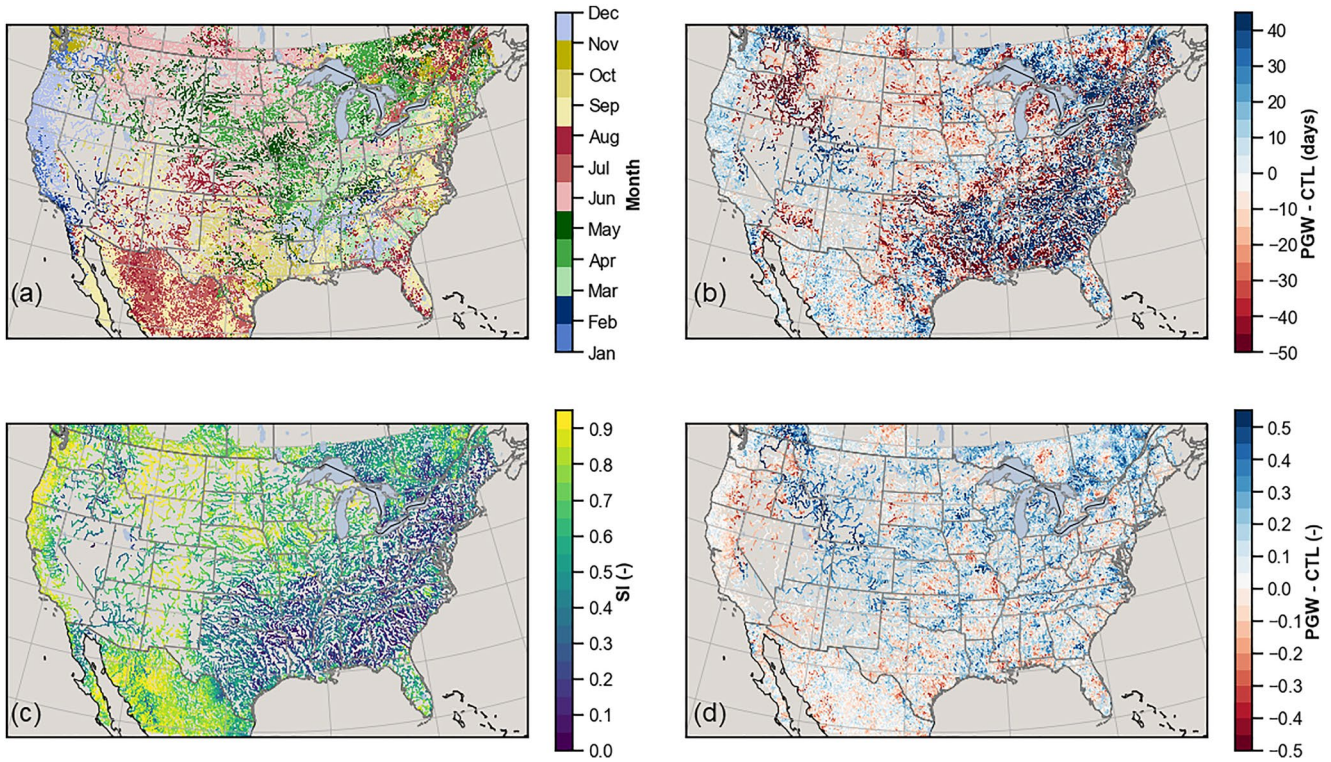

Figure 8. Similar to Figure 6, but for floods.

while rainfall and flooding events become more correlated. Both correlations can act as predictive tools to infer future flood characteristics.

Breaking down the correlations into months in Figure 10e, we can diagnose the monthly correlation variations. We observe the correlation of rainfall-flood date in PGW is apparently higher in the future for the cool seasons (January, February, March, and April). Correlation is nearly zero for CTL simulation in these months because of

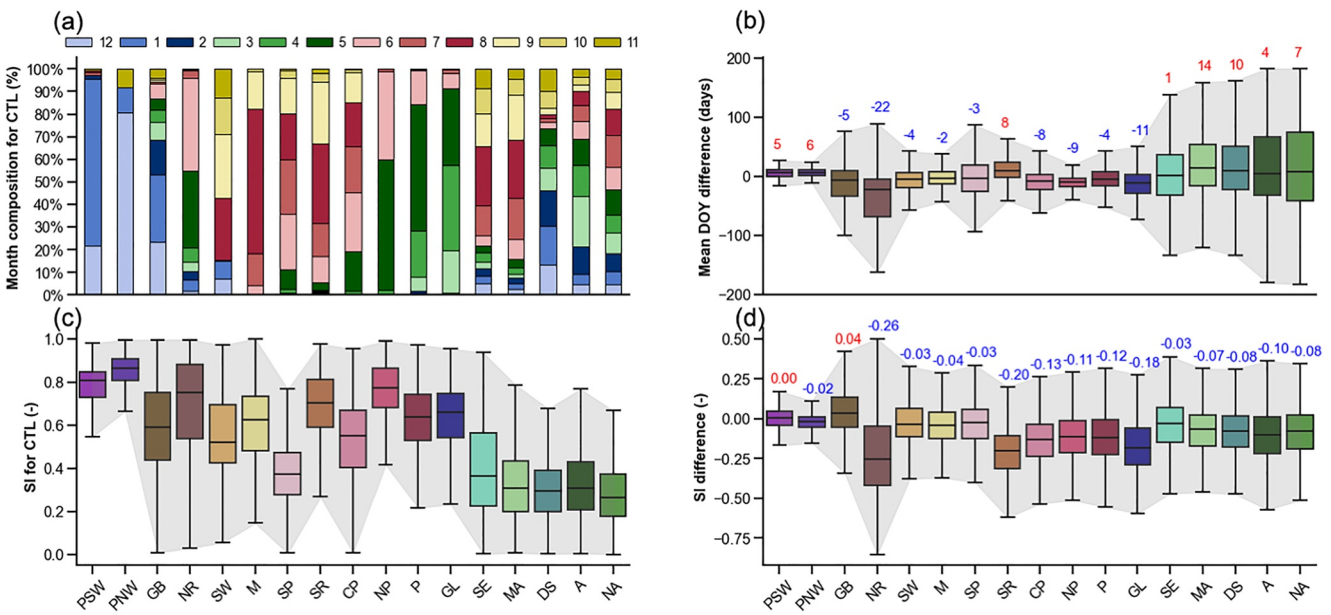

Figure 9. Similar to Figure 7, but for floods.

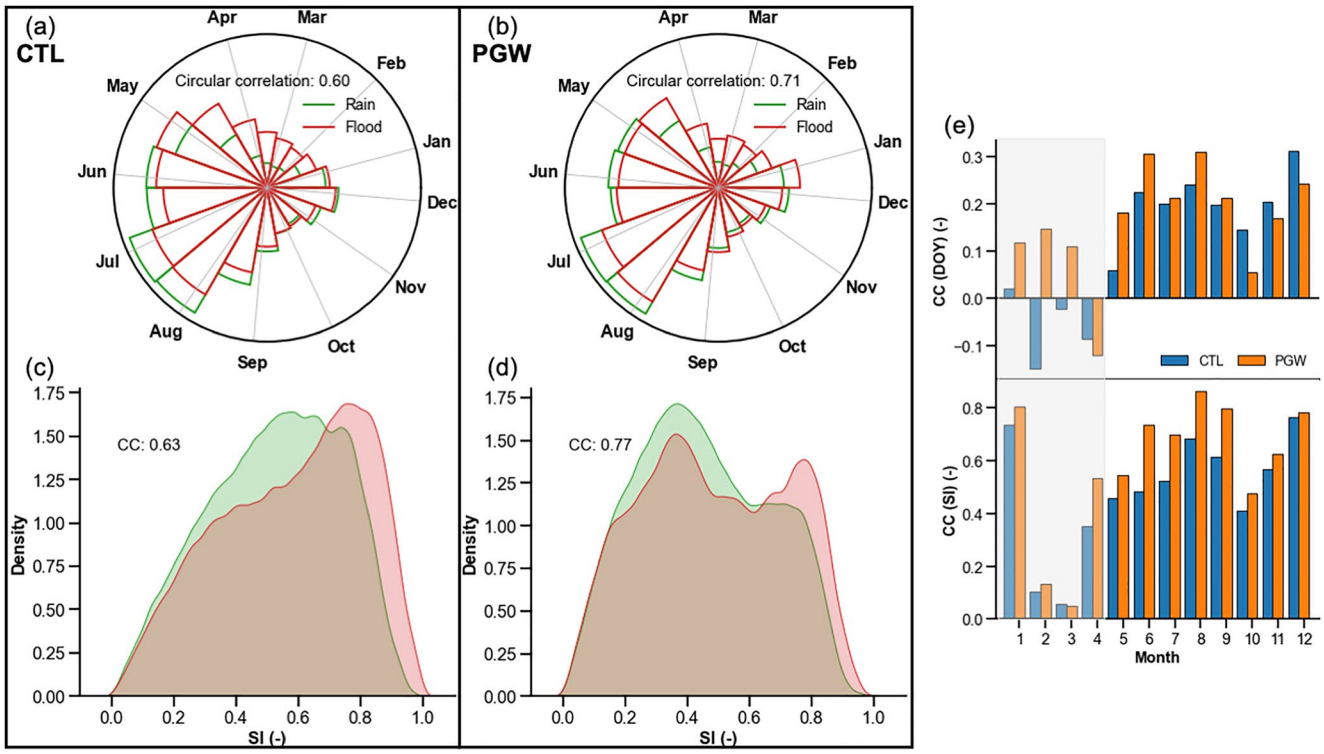

Figure 10. Temporal correction between rainfall and floods: (a) circular correlation in rainfall-flooding date in historical simulation; (b) circular correlation in rainfall-flooding date in future simulation; (c) histogram of seasonality index in historical simulation; (d) histogram of seasonality index in future simulation; (e) correlations of Date of Year and seasonality index by month.

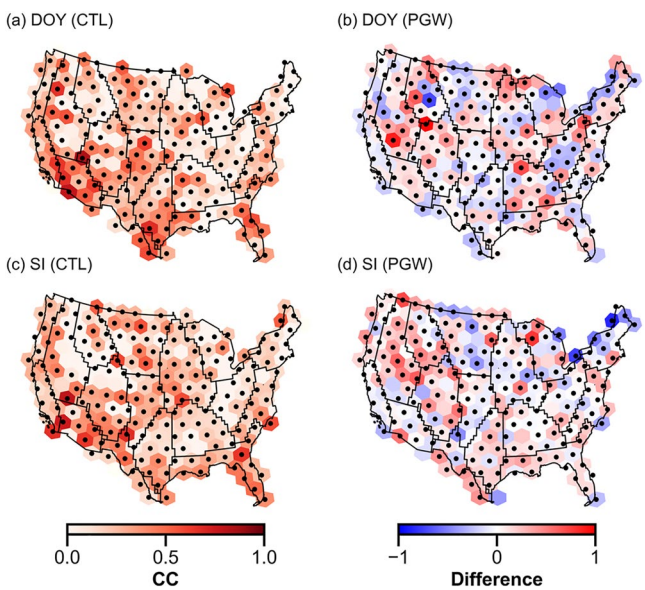

Figure 11. Map of correlation over the CONUS: (a) circular correlation between rainfall and flood dates in CTL simulation; (b) differences of circular correlation between rainfall and flood dates (Pseudo Global Warming [PGW]-CTL); (c) Spearman correlation between rainfall and flood seasonality in CTL simulation; (d) differences of spearman correlation between rainfall and flood seasonality (PGW-CTL). The stipples indicate a significant correlation (p-value less than 0.05) between rainfall and flood.

the delayed rainfall-runoff process. However, earlier snowmelt in the future shortens that delay, thereby leading to a higher correlation (~0.1). On the other hand, the present-day correlations in October, November, and December are slightly higher than those in PGW. The correlation of seasonality in the future is consistently higher than present across months, while the correlations in February and March for both CTL and PGW are small (0.1).

The spatial map showing a rainfall-flood correlation in Figure 11 identifies regions with strong/weak correlations. The rainfall-flood date correlation is generally stronger in the western US (0.31) than in the eastern US (0.11). The Southwest and Mezquital, in particular, have CC values above 0.6 because of intense storms and low-infiltrating soils, resulting in flashy floods. This correlation even becomes 14.9% stronger in the future, possibly due to intensified storms fueled by enhanced temperature (energy) and atmospheric moisture (water availability). The Great Basin and Rockies will also have 34.4% higher correlations in the future, which is related to earlier snowmelt that reduces rainfall-runoff lag time. The central and eastern US have slight increases in the correlation of DOY. The correlation of seasonality is increased across the CONUS, except for the Great Lakes, Prairie, and North-Atlantic.

4. Discussion

4.1. Representativeness of Flood Synchrony Scale by Hydrologic Models

This study introduces a new method that uses a high-resolution distributed hydrologic model to overcome limited coverages by stream gauges that are

conventionally used to derive flood synchrony scale (Berghuijs et al., 2019; Brunner et al., 2020). The added values of model simulation against stream gauges are two-fold. First, in terms of spatial extent, the reach-scale representation of flood enabled by modeling is more informative than stream gauges at point-scale. In a simple illustration (Figure S4 in Supporting Information S1), let us assume gauge-based approach indicates flood synchrony at A, B, C, and D with near-perfect confidence, despite the inherent uncertainty sources from subjective parameterization and gauge measurement itself. Such confidence probably drops quickly as the target of estimation moves away from these gauge points. Put simply, one may argue the reaches in between these gauges have synchronous floods, but it would be hard for him/her to infer the extent outside these gauges. In comparison, the level of confidence at gauge locations and their contributing area is comparable. Moreover, we can now not only infer synchronous floods occurred between A–B, B–C, and C–D as a way of interpolation but also at extended reaches that is, A–E, D–F, and B–G. In essence, the modeling approach can be seen as a way to physically interpolate/extrapolate information from gauges.

The second fold is whether model simulated flood synchrony is realistic, which necessitates careful validation. We gathered flow frequency data at more than 6,000 USGS gauges and compared simulated 2-year flow with observed values (Figure S5 in Supporting Information S1). The underestimation of 2-year flow is obvious, with the bias being −1.1. Further, the validity of spatially synchronous flood is verified using a metric connectedness error (Figure S6 in Supporting Information S1), which measures the differences between number of gauges by simulation and by observation co-experiencing floods. Overall, the median connectedness error is centered around zero, with slight underestimation (−16). Particularly for spring floods, the degree of underestimation is magnified (−121). The overall underestimation of both 2-year flow and synchronous flood events point to an overall dry bias, as reported by Liu et al. (2017) and Li et al. (2022).

However, such validation is difficult to directly assess the flood synchrony scale by observations and simulations. Spatially coherent observation is more insightful. A collection of satellite observations such as optical sensors (e.g., MODIS, Landsat) and synthetical aperture radars (e.g., Sentinel-1) is promising to construct a flood synchrony data set for model validation. In this study, we instead emphasize the relative changes due to climate change while did not conduct full-blown evaluation.

4.2. Sensitivity of the Results to Climate Divisions and Extreme Thresholds

Results interpreted in this study are subject to choices of climate divisions and thresholds to determine extreme rainfall or floods. The Bukovsky climate zones, relative to the Koppen-Geiger climate zones, are assumed to be more homogenous. We expect the zonal mean statistics calculated in for example, Figures 3 and 5 can vary as if using different climate divisions. However, the general message should be similar—western US will likely experience greater changes in floods yet less changes in extreme rainfall, as counter to the eastern US. Second, the extreme thresholds for rainfall and floods have great impacts on occurrences of those events. A detailed depiction of extreme rainfall and flooding events such as low-end and high-end extreme events is insightful to cover the full spectrum of frequency. This study establishes a methodology and paves a way for future research on such a scope.

4.3. Results Intercomparison

Despite many existing climate studies that focus on flooding, few of them have fully considered convective-scale storms based on the GCM, which forms the foundational differences when making comparisons. For instance, previous studies indicate that some dry regions such as the Southwest will experience less frequent floods (Hirabayashi et al., 2013), However, we see an increase in flood frequency and scales (Figure 5). This contrasting result is likely a reflection of different climate data at different scales. First, our high-resolution climate simulation can overcome the poor representation of extreme precipitation (especially convective-scale storms) in GCMs that are often used in large-scale flood simulation (Farnham et al., 2018; Kendon et al., 2012). Second, this data set is primarily used for assessing thermodynamic changes in the atmosphere, which exerts great importance in invigorating storms in the future, while the dynamic changes included in other flood studies are not allowed. Some similarities coexist with differences. For instance, intensification of extreme rainfall and flood events with respect to their spatial scales is found in Yu et al. (2020). Earlier flood onsetting over the Rockies and later in the eastern US have been supported by other studies (Li, Chen, Gao, Gourley, et al., 2021; Villarini, 2016; Xu et al., 2021).

4.4. Reconciling Different Rainfall-Flood Patterns in the Western and Eastern US

Floods are modulated not only by the atmosphere and climate mechanisms but also catchment states (e.g., antecedent soil moisture, groundwater level, land-use changes, snowmelt, and rain on snow) and river networks (Merz et al., 2021). In this study, we found different patterns for the changes in extreme rainfall and floods across the US. The western US is likely to experience greater (less) changes in flood (rainfall) frequency and spatial scales, as opposed to eastern US whose changes in rainfall (flood) frequency and spatial scales are greater (lesser). One plausible reason is the changes in antecedent soil moisture. To verify whether the future catchment state is drying, especially in the eastern US, we extracted antecedent soil moisture, 1 day prior to the onset of flooding events, as shown in Figure S7 in Supporting Information S1. Distinct spatial patterns appear in Figure S7a in Supporting Information S1—higher values in the eastern US and lower in the western US. In the future, there is a drying tendency of antecedent soil moisture conditions over a large portion of the US, especially in the Southern Plains. The eastern US generally experiences 0%–5% drier soil moisture conditions in the future, in contrast to 5%–10% wetter in the Pacific Coast and Great Basin (Figure S7b in Supporting Information S1). It explains why the future increase in rainfall extent is more closely tied to flood extent in the West than the East, as the dry antecedent soils modulate the intense rainfall.

5. Conclusion

In this study, we explore the spatiotemporal patterns of US floods under the current climate and how they change under a warmer climate. A convection-permitting climate simulation enables high-resolution flood simulation (CREST model + Snow 17 model), which reveals a continental perspective of reach-level flood spatiotemporal characteristics. The following points summarize the primary findings of the study:

1. In the future climate scenario, the 2-year rainfall occurrences and spatial scales increase by 118.0% and 101.7%, respectively. As a consequence, the 2-year flood occurrences and spatial scales increase by 101.7% and 44.9% across the US.
2. Earlier and Faster snowmelt bring earlier flood season onset and shorten rainfall-to-flood timing, which results in 0.11 and 0.14 stronger correlation in date of occurrence and seasonality.
3. Regionally, floods in the western US become relatively more severe (+70.6% greater flood spatial scale) in the future than those in the East (+35.8% greater flood spatial scale), as snowmelt exacerbates flooding in the West, while the drier antecedent catchment soil moisture in the East partially offsets flooding.
4. The Pacific Coast, both currently and in the future, has the strongest seasonality for extreme rainfall (0.80) and floods (0.85) in the US However, seasonality decreases moving toward the East Coast (0.4 for rainfall and 0.3 for floods). The seasonal cycles of rainfall and floods become less pronounced in the East, partly caused by more evenly distributed extreme rainfall days, earlier snowmelt, and lengthened rainfall-runoff lag time in watersheds with drier soils in the future.

This study reveals a pressing need for the national weather and hydrology community to adapt to climate change because of not only intensified frequency in rainfall and floods but also more widespread rainfall and floods. Even worse, the weakening seasonal cycle of extreme rainfall and floods challenges flood predictability asnd preparedness. We recommend future works incorporating anthropogenic effects on floods in detail to present an economic assessment of future flood damages and resilience measures.

Conflict of Interest

The authors declare no conflicts of interest relevant to this study.

Data Availability Statement

The climate simulation data (Liu et al., 2017) is downloaded from the National Center for Atmospheric Research (NCAR) Research Data Archive (https://rda.ucar.edu/datasets/ds612.0). The EF5/CREST model (Flamig, 2020) is publicly available from Zenodo https://doi.org/10.5281/zenodo.4009759 and Github https://github.com/HyDROSLab/EF5.

Acknowledgments
We would like to acknowledge the efforts by research team at the National Center for Atmospheric Research (NCAR) for making the climate simulation data publicly available on NCAR's High Performance Storage System (https://rda.ucar.edu/datasets/ds612.0/). The first author is sponsored by the University of Oklahoma Hydrology and Water Security (HWS) program (https://www.ouhydrologyonline.com/) and Graduate College Hoving Fellowship.

References

Alfieri, L., Dottori, F., Salamon, P., Wu, H., & Feyen, L. (2020). Global modeling of seasonal mortality rates from river floods. *Earth's Future*, *8*, e2020EF001541. https://doi.org/10.1029/2020EF001541

Ashley, W. S., Mote, T. L., Dixon, P. G., Trotter, S. L., Powell, E. J., Durkee, J. D., & Grundstein, A. J. (2003). Distribution of mesoscale convective complex rainfall in the United States. *Monthly Weather Review*, *131*(12), 3003–3017.

Barbero, R., Abatzoglou, J. T., & Fowler, H. J. (2019). Contribution of large-scale midlatitude disturbances to hourly precipitation extremes in the United States. *Climate Dynamics*, *52*, 197–208. https://doi.org/10.1007/s00382-018-4123-5

Bates, P. D., Quinn, N., Sampson, C., Smith, A., Wing, O., Sosa, J., et al. (2020). Combined modelling of US fluvial, pluvial and coastal flood hazard under current and future climates. *Water Resources Research*, *56*, e2020WR028673.

Berghuijs, W. R., Allen, S. T., Harrigan, S., & Kirchner, J. W. (2019). Growing spatial scales of synchronous river flooding in Europe. *Geophysical Research Letters*, *46*, 1423–1428. https://doi.org/10.1029/2018GL081883

Blöschl, G., Hall, J., Parajka, J., Perdigão, R. A. P., Merz, B., Arheimer, B., et al. (2017). Changing climate shifts timing of European floods. *Science*, *357*(6351), 588–590. https://doi.org/10.1126/science.aan2506

Brunner, M. I., Gilleland, E., Wood, A., Swain, D. L., & Clark, M. (2020). Spatial dependence of floods shaped by spatiotemporal variations in meteorological and land-surface processes. *Geophysical Research Letters*, *47*, e2020GL088000. https://doi.org/10.1029/2020GL088000

Brunner, M. I., Swain, D. L., Wood, R. R., Willkofer, F., Done, J. M., Gilleland, E., & Ludwig, R. (2021). An extremeness threshold determines the regional response of floods to changes in rainfall extremes. *Communications Earth and Environment*, *2*, 173. https://doi.org/10.1038/s43247-021-00248-x

Bukovsky, M. S. (2011). *Masks for the Bukovsky regionalization of North America, Regional Integrated Sciences Collective*. Institute for Mathematics Applied to Geosciences, National Center for Atmospheric Research. Downloaded 2021-07-05. Retrieved from http://www.narccap.ucar.edu/contrib/bukovsky/

Burn, D. H. (1997). Catchment similarity for regional flood frequency analysis using seasonality measures. *Journal of Hydrology*, *202*, 212–230. https://doi.org/10.1016/S0022-1694(97)00068-1

Chalise, D. R., Aiyyer, A., & Sankarasubramanian, A. (2021). Tropical cyclones' contribution to seasonal precipitation and streamflow over the southeastern and southcentral United States. *Geophysical Research Letters*, *48*(15), e2021GL094738. https://doi.org/10.1029/2021GL094738

Chen, M., Li, Z., Gao, S., Luo, X., Wing, O. E. J., Shen, X., et al. (2021). A comprehensive flood inundation mapping for hurricane harvey using an integrated hydrological and hydraulic model. *Journal of Hydrometeorology*, *22*(7), 1713–1726. https://doi.org/10.1175/jhm-d-20-0218.1

Clark, M. P., Wilby, R. L., Gutmann, E. D., Vano, J. A., Gangopadhyay, S., Wood, A., et al. (2016). Characterizing uncertainty of the hydrologic impacts of climate change. *Current Climate Change Reports*, *2*, 55–64. https://doi.org/10.1007/s40641-016-0034-x

Dougherty, E., & Rasmussen, K. L. (2020). Changes in future flash flood–producing storms in the United States. *Journal of Hydrometeorology*, *21*, 2221–2236. https://doi.org/10.1175/jhm-d-20-0014.1

Douville, H., Raghavan, K., Renwick, J., Allan, R. P., Arias, P. A., Barlow, M., et al. (2021). Water cycle changes. In P. Zhai, A. Pirani, S. L. Connors, C. Péan, S. Berger, N. Caud, et al. (Eds.), *Climate change 2021: The physical science basis. Contribution of working group I to the sixth assessment report of the intergovernmental panel on climate change [Masson-Delmotte, V.]*. Cambridge University Press.

Ester, M., Kriegel, H. P., Sander, J., & Xu, X. (1996). A density-based algorithm for discovering clusters in large spatial databases with noise. *KDD*, *96*, 226–231.

Farnham, D. J., Doss-Gollin, J., & Lall, U. (2018). Regional extreme precipitation events: Robust inference from credibly simulated GCM variables. *Water Resources Research*, *54*, 3809–3824. https://doi.org/10.1002/2017WR021318

Feng, Z., Leung, L., Hagos, S., Houze, R. A., Burleyson, C. D., & Balaguru, K. (2016). More frequent intense and long-lived storms dominate the springtime trend in central US rainfall. *Nature Communications*, *7*, 13429. https://doi.org/10.1038/ncomms13429

Flamig, Z. (2020). HyDROSLab/EF5-US-Parameters: EF5 parameters for USA (v1.0.0). *Zenodo*. https://doi.org/10.5281/zenodo.4009759

Flamig, Z. L., Vergara, H., & Gourley, J. J. (2020). The ensemble framework for flash flood forecasting (EF5) v1.2: Description and case study. *Geoscientific Model Development*, *13*(10), 4943–4958. https://doi.org/10.5194/gmd-13-4943-2020

Fritsch, J. M., Kane, R. J., & Chelius, C. R. (1986). The contribution of mesoscale convective weather systems to the warm-season precipitation in the United States. *Journal of Applied Meteorology and Climatology*, *25*, 1333–1345. https://doi.org/10.1175/1520-0450(1986)025<1333:tcomcw>2.0.co;2

Giuntoli, I., Prosdocimi, I., & Hannah, D. M. (2021). Going beyond the ensemble mean: Assessment of future floods from global multi-models. *Water Resources Research*, *57*, e2020WR027897. https://doi.org/10.1029/2020WR027897

Gourley, J. J., Flamig, Z. L., Vergara, H., Kirstetter, P., Clark, R. A., Argyle, E., et al. (2017). The FLASH Project: Improving the tools for flash flood monitoring and prediction across the United States. *Bulltin of the American Meteorlogical Society*, *98*, 361–372. https://doi.org/10.1175/BAMS-D-15-00247.1

Hagos, S. M., Leung, L. R., Yoon, J.-H., Lu, J., & Gao, Y. (2016). A projection of changes in landfalling atmospheric river frequency and extreme precipitation over western North America from the Large Ensemble CESM simulations. *Geophysical Research Letters*, *43*, 1357–1363. https://doi.org/10.1002/2015GL067392

He, L., & Wilkerson, G. V. (2011). Improved bankfull channel geometry prediction using two-year return-period discharge. *Journal of the American Water Resources Association*, *47*, 1298–1316. https://doi.org/10.1111/j.1752-1688.2011.00567.x

Hirabayashi, Y., Mahendran, R., Koirala, S., Konoshima, L., Yamazaki, D., Watanabe, S., et al. (2013). Global flood risk under climate change. *Nature Climate Change*, *3*, 816–821. https://doi.org/10.1038/nclimate1911

Ivancic, T. J., & Shaw, S. B. (2015). Examining why trends in very heavy precipitation should not be mistaken for trends in very high river discharge. *Climatic Change*, *133*, 681–693. https://doi.org/10.1007/s10584-015-1476-1

Jongman, B., Ward, P., & Aerts, J. C. J. H. (2012). Global exposure to river and coastal flooding: Long term trends and changes. *Global Environmental Change*, *22*, 823–835. https://doi.org/10.1016/j.gloenvcha.2012.07.004

Kemter, M., Merz, B., Marwan, N., Vorogushyn, S., & Blöschl, G. (2020). Joint trends in flood magnitudes and spatial extents across Europe. *Geophysical Research Letters*, *47*, e2020GL087464. https://doi.org/10.1029/2020GL087464

Kendon, E. J., Roberts, N. M., Senior, C. A., & Roberts, M. J. (2012). Realism of rainfall in a very high-resolution regional climate model. *Journal of Climate*, *25*(17), 5791–5806. https://doi.org/10.1175/JCLI-D-11-00562.1

Lamjiri, M. A., Dettinger, M. D., Ralph, F. M., & Guan, B. (2017). Hourly storm characteristics along the US West Coast: Role of atmospheric rivers in extreme precipitation. *Geophysical Research Letters*, *44*, 7020–7028. https://doi.org/10.1002/2017GL074193

Ledingham, J., Archer, D., Lewis, E., Fowler, H., & Kilsby, C. (2019). Contrasting seasonality of storm rainfall and flood runoff in the UK and some implications for rainfall-runoff methods of flood estimation. *Hydrology Research*, *50*(5), 1309–1323. https://doi.org/10.2166/nh.2019.040

Li, Z., Chen, M., Gao, S., Gourley, J. J., Yang, T., Shen, X., et al. (2021). A multi-source 120-year US flood database with a unified common format and public access. *Earth System Science Data*, *13*, 3755–3766. https://doi.org/10.5194/essd-2021-36

Li, Z., Chen, M., Gao, S., Luo, X., Gourley, J. J., Kirstetter, P., et al. (2021). CREST-iMAP v1. 0: A fully coupled hydrologic-hydraulic modeling framework dedicated to flood inundation mapping and prediction. *Environmental Modelling & Software*, *141*, 105051. https://doi.org/10.1016/j.envsoft.2021.105051

Li, Z., Gao, S., Chen, M., Gourley, J. J., Liu, C., Prein, A., & Hong, Y. (2022). The conterminous United States are projected to become more prone to flash floods in a high-end emissions scenario. *Communications Earth & Environment*, *3*, 86. https://doi.org/10.1038/s43247-022-00409-6

Li, Z., Yang, Y., Kan, G., & Hong, Y. (2018). Study on the applicability of the Hargreaves potential evapotranspiration estimation method in CREST distributed hydrological model (version 3.0) Applications. *Water*, *10*, 1882. https://doi.org/10.3390/w10121882

Liu, C., Ikeda, K., Rasmussen, R., Barlage, M., Newman, A. J., Prein, A. F., et al. (2017). Continental-scale convection-permitting modeling of the current and future climate of North America. *Climate Dynamics*, *49*(1–2), 71–95. https://doi.org/10.1007/s00382-016-3327-9

Merz, B., Blöschl, G., Vorogushyn, S., Dottori, F., Aerts, J. C. J. H., Bates, P., et al. (2021). Causes, impacts and patterns of disastrous river floods. *Nature Reviews Earth & Environment*, *2*(9), 592–609. https://doi.org/10.1038/s43017-021-00195-3

Musselman, K. N., Lehner, F., Ikeda, K., Clark, M., Prein, A., Liu, C., et al. (2018). Projected increases and shifts in rain-on-snow flood risk over western North America. *Nature Climate Change*, *8*, 808–812. https://doi.org/10.1038/s41558-018-0236-4

Nie, J., Sobel, A. H., Shaevitz, D. A., & Wang, S. (2018). Dynamic amplification of extreme precipitation sensitivity. *Preceedings of the National Academy of Sciences of the United States of America*, *115*, 9467–9472. https://doi.org/10.1073/pnas.1800357115

Prein, A. F., Liu, C., Ikeda, K., Trier, S. B., Rasmussen, R. M., Holland, G. J., & Clark, M. (2017). Increased rainfall volume from future convective storms in the US. *Nature Climate Change*, *7*, 880–884. https://doi.org/10.1038/s41558-017-0007-7

Prein, A. F., & Mearns, L. O. (2021). US Extreme precipitation weather types increased in frequency during the 20th century. *Journal of Geophysical Research: Atmospheres*, *126*, e2020JD034287. https://doi.org/10.1029/2020JD034287

Rajib, A., Zheng, Q., Golden, H. E., Wu, Q., Lane, C. R., Christensen, J. R., et al. (2021). The changing face of floodplains in the Mississippi River Basin detected by a 60-year land use change dataset. *Scientific Data*, *8*, 271. https://doi.org/10.1038/s41597-021-01048-w

Schär, C., Frei, C., Lüthi, D., & Davies, H. C. (1996). Surrogate climate-change scenarios for regional climate models. *Geophysical Research Letters*, *23*, 669–672. https://doi.org/10.1029/96gl00265

Sharma, A., Wasko, C., & Lettenmaier, D. P. (2018). If precipitation extremes are increasing, why aren't floods? *Water Resources Research*, *54*(11), 8545–8551. https://doi.org/10.1029/2018WR023749

Smith, J. A., Villarini, G., & Baeck, M. L. (2011). Mixture distributions and the climatology of extreme rainfall and flooding in the Eastern US. *Journal of Hydrometeorology*, *12*(2), 294–309.

Stein, L., Clark, M. P., Knoben, W. J. M., Pianosi, F., & Woods, R. A. (2021). How do climate and catchment attributes influence flood generating processes? A large-sample study for 671 catchments across the contiguous USA. *Water Resources Research*, *57*, e2020WR028300. https://doi.org/10.1029/2020WR028300

Swain, D. L., Wing, O. E. J., Bates, P. D., Done, J. M., Johnson, K. A., & Cameron, D. R. (2020). Increased flood exposure due to climate change and population growth in the United States. *Earth's Future*, *8*, e2020EF001778. https://doi.org/10.1029/2020ef001778

Tellman, B., Sullivan, J. A., Kuhn, C., Kettner, A. J., Doyle, C. S., Brakenridge, G. R., et al. (2021). Satellite imaging reveals increased proportion of population exposed to floods. *Nature*, *596*, 80–86. https://doi.org/10.1038/s41586-021-03695-w

Thornthwaite, C. W. (1948). An approach toward a rational classification of climate. *Geographical Review*, *38*, 55–94. https://doi.org/10.2307/210739

Veilleux, A. G., Cohn, T. A., Flynn, K. M., Mason, R. R., & Hummel, P. R. (2014). *Estimating magnitude and frequency of floods using the PeakFQ 7.0 program*. U.S. Geological Survey Fact Sheet 2013–3108. https://doi.org/10.3133/fs20133108

Vergara, H., Kirstetter, P., Gourley, J. J., Flamig, Z. L., Hong, Y., Arthur, A., & Kolar, R. (2016). Estimating a-priori kinematic wave model parameters based on regionalization for flash flood forecasting in the Conterminous United States. *Journal of Hydrology*, *541*, 421–433. https://doi.org/10.1016/j.jhydrol.2016.06.011

Villarini, G. (2016). On the seasonality of flooding across the continental United States. *Advances in Water Research*, *87*, 80–91. https://doi.org/10.1016/j.advwatres.2015.11.009

Wasko, C., Nathan, R., Stein, L., & O'Shea, D. (2021). Evidence of shorter more extreme rainfalls and increased flood variability under climate change. *Journal of Hydrology*, *603*, 126994. https://doi.org/10.1016/j.jhydrol.2021.126994

Wasko, C., & Sharma, A. (2017). Global assessment of flood and storm extremes with increased temperatures. *Scientific Reports*, *7*, 7945. https://doi.org/10.1038/s41598-017-08481-1

Wasko, C., Sharma, A., & Lettenmaier, D. P. (2019). Increases in temperature do not translate to increased flooding. *Nature Communications*, *10*, 5676. https://doi.org/10.1038/s41467-019-13612-5

Wu, H., Adler, R. F., Hong, Y., Tian, Y., & Policelli, F. (2012). Evaluation of global flood detection using satellite-based rainfall and a hydrologic model. *Journal of Hydrometeorology*, *13*(4), 1268–1284.

Xu, D., Ivanov, V. Y., Li, X., & Troy, T. J. (2021). Peak runoff timing is linked to global warming trajectories. *Earth's Future*, *9*, e2021EF002083. https://doi.org/10.1029/2021EF002083

Yu, G., Wright, D. B., & Li, Z. (2020). The upper tail of precipitation in convection-permitting regional climate models and their utility in nonstationary rainfall and flood frequency analysis. *Earth's Future*, *8*, e2020EF001613. https://doi.org/10.1029/2020EF001613

Zhang, K., Xue, X., Hong, Y., Gourley, J. J., Lu, N., Wan, Z., et al. (2016). iCRESTRIGRS: A coupled modeling system for cascading flood–landslide disaster forecasting. *Hydrology and Earth System Sciences*, *20*, 5035–5048. https://doi.org/10.5194/hess-20-5035-2016